SUSY dark matter in light of CDMS II results: a comparative study for different models

Junjie Cao[1], Ken-ichi Hikasa[2], Wenyu Wang[3], Jin Min Yang[4], Li-Xin Yu[4]

[1] *Department of Physics, Henan Normal university, Xinxiang 453007, China*
[2] *Department of Physics, Tohoku University, Sendai 980-8578, Japan*
[3] *Institute of Theoretical Physics, College of Applied Science, Beijing University of Technology, Beijing 100124, China*
[4] *Key Laboratory of Frontiers in Theoretical Physics, Institute of Theoretical Physics, Academia Sinica, Beijing 100190, China*

We perform a comparative study of the neutralino dark matter scattering on nucleon in three popular supersymmetric models: the minimal (MSSM), the next-to-minimal (NMSSM) and the nearly minimal (nMSSM). First, we give the predictions of the elastic cross section by scanning over the parameter space allowed by various direct and indirect constraints, which are from the measurement of the cosmic dark matter relic density, the collider search for Higgs boson and sparticles, the precision electroweak measurements and the muon anomalous magnetic moment. Then we demonstrate the property of the allowed parameter space with/without the new limits from CDMS II. We obtain the following observations: (i) For each model the new CDMS limits can exclude a large part of the parameter space allowed by current collider constraints; (ii) The property of the allowed parameter space is similar for MSSM and NMSSM, but quite different for nMSSM; (iii) The future SuperCDMS can cover most part of the allowed parameter space for each model.

PACS numbers: 14.80.Cp,12.60.Fr,11.30.Qc

I. INTRODUCTION

Although there are many theoretical or aesthetical arguments for the necessity of TeV-scale new physics, the most convincing evidence is from the WMAP (Wilkinson Microwave Anisotropy Probe) observation of the cosmic cold dark matter, which naturally indicate the existence of WIMPs (Weakly Interacting Massive Particle) beyond the prediction of the Standard Model (SM). By contrast, the neutrino oscillation may rather imply trivial new physics (plainly adding right-handed neutrinos to the SM) or new physics at some very high see-saw scale unaccessible to any foreseeable colliders. Therefore, the TeV-scale new physics to be unravelled at the Large Hadron Collider (LHC) is most likely related to the WIMP dark matter.

If WIMP dark matter is chosen by nature, then it will naturally direct to low-energy supersymmetry (SUSY) with R-parity although other miscellaneous speculations are also possible. In addition to the perfect explanation of cosmic dark matter, to make perfection still more perfect, SUSY can also solve another plausible puzzle, namely the 3σ deviation of the muon anomalous magnetic moment from the SM prediction. In the framework of SUSY, the most intensively studied model is the minimal supersymmetric standard model (MSSM) [1], which is the most economical realization of SUSY. Since this model suffers from the μ-problem and the little hierarchy problem, other supersymmetric models have recently attracted much attention, among which is the extension by introducing a gauge singlet superfield $\hat{S}$, such as the next-to-minimal supersymmetric model (NMSSM) [2] and the nearly minimal supersymmetric model (nMSSM) [3, 4]. In addition to the attractive phenomenological virtues like the alleviation of the little hierarchy problem and the possible explanation [5] of PAMELA positron excess (albeit subject to large uncertainty and could be explained astrophysically by pulsars) [6], such singlet extensions are arguably motivated by some fancy string theory, e.g., the NMSSM can be constructed from a heterotic string [7].

In this work, motivated by the CDMS II new results [8, 9], we examine the SUSY dark matter scattering on the nucleon (χ-nucleon scattering). In the literature such a topic has been studied mainly in the constrained MSSM [10]. Our work is projected to have the following features:

(i) We perform a comparative study for three popular SUSY models: the MSSM, the NMSSM and the nMSSM.

(ii) We consider the constraints from the cosmic dark matter relic density and current collider experiments, such as the collider search for Higgs boson and sparticles, the precision electroweak measurements and the muon anomalous magnetic moment. By scanning over the parameter space subject to these constraints, for each model we find out the allowed parameter space and give the predictions of the cross section for χ-nucleon scattering with comparison to the CDMS II results.

(iii) We demonstrate the properties of the allowed parameter space (such as the components of the neutralino dark matter and the invisible Higgs boson decay into a pair of dark matter particles) by comparing the three models.

(iv) We show the capability of the SuperCDMS [11] in probing the currently allowed parameter space for each model.

This paper is organized as follows. In Sec.II we briefly describe the three models: the MSSM, the NMSSM and the nMSSM, focusing on the Higgs sector and the neutralino/chargino sector since they are directly relevant to the dark matter scattering. In Sec.III we scan over the parameter space under current constraints, and give the predictions of the cross section for χ-nucleon scattering with comparison to the CDMS II results. Also we will demonstrate the properties of the allowed parameter space with/without considering the CDMS new limits. In Sec. IV we give our conclusions.

II. SUPERSYMMETRIC MODELS

As the economical realizations of supersymmetry, the MSSM has the minimal content of particles, while the NMSSM and nMSSM extend the MSSM by only adding one singlet Higgs superfield $\hat{S}$. The difference between these models is reflected in their superpotential:

$$W_{\rm MSSM} = W_F + \mu \hat{H}_u \cdot \hat{H}_d, \tag{1}$$

$$W_{\rm NMSSM} = W_F + \lambda \hat{H}_u \cdot \hat{H}_d \hat{S} + \frac{1}{3}\kappa \hat{S}^3, \tag{2}$$

$$W_{\rm nMSSM} = W_F + \lambda \hat{H}_u \cdot \hat{H}_d \hat{S} + \xi_F M_n^2 \hat{S}, \tag{3}$$

where $W_F = Y_u \hat{Q} \cdot \hat{H}_u \hat{U} - Y_d \hat{Q} \cdot \hat{H}_d \hat{D} - Y_e \hat{L} \cdot \hat{H}_d \hat{E}$ with $\hat{Q}$, $\hat{U}$ and $\hat{D}$ being the squark superfields, and $\hat{L}$ and $\hat{E}$ being the slepton superfields, $\hat{H}_u$ and $\hat{H}_d$ are the Higgs doublet superfields, λ, κ and ξ_F are dimensionless coefficients, and μ and M_n are parameters with mass dimension. Note that there is no explicit μ-term in the NMSSM or nMSSM, and an effective μ-parameter can be generated when the scalar component (S) of $\hat{S}$ develops a vev (vacuum expectation value). Also note that the nMSSM differs from the NMSSM in the last term with the trilinear singlet term $\kappa \hat{S}^3$ of the NMSSM replaced by the tadpole term $\xi_F M_n^2 \hat{S}$. As pointed out in [3], such a tadpole term can be generated at a high loop level and naturally be of the SUSY breaking scale. The advantage of such replacement is the nMSSM has no discrete symmetry and thus free of the domain wall problem which the NMSSM suffers from.

Corresponding to the superpotential, the Higgs soft terms in the scalar potentials are also different for three models (the soft terms for gauginos and sfermions are the same and not listed here)

$$V_{\rm soft}^{\rm MSSM} = \tilde{m}_d^2 |H_d|^2 + \tilde{m}_u^2 |H_u|^2 + (B\mu H_u \cdot H_d + \text{h.c.}) \tag{4}$$

$$V_{\rm soft}^{\rm NMSSM} = \tilde{m}_d^2 |H_d|^2 + \tilde{m}_u^2 |H_u|^2 + \tilde{m}_s^2 |S|^2 + \left(A_\lambda \lambda S H_d \cdot H_u + \frac{\kappa}{3} A_\kappa S^3 + \text{h.c.} \right), \tag{5}$$

$$V_{\rm soft}^{\rm nMSSM} = \tilde{m}_d^2 |H_d|^2 + \tilde{m}_u^2 |H_u|^2 + \tilde{m}_s^2 |S|^2 + \left(A_\lambda \lambda S H_d \cdot H_u + \xi_S M_n^3 S + \text{h.c.} \right). \tag{6}$$

After the scalar fields H_u,H_d and S develop their vevs v_u, v_d and s respectively, they can be expanded as

$$H_d = \begin{pmatrix} \frac{1}{\sqrt{2}}(v_d + \phi_d + i\varphi_d) \\ H_d^- \end{pmatrix}, H_u = \begin{pmatrix} H_u^+ \\ \frac{1}{\sqrt{2}}(v_u + \phi_u + i\varphi_u) \end{pmatrix}, S = \frac{1}{\sqrt{2}}(s + \sigma + i\xi). \tag{7}$$

The mass eigenstates can be obtained by unitary rotations

$$\begin{pmatrix} H_1 \\ H_2 \\ H_3 \end{pmatrix} = U^H \begin{pmatrix} \phi_d \\ \phi_u \\ \sigma \end{pmatrix}, \quad \begin{pmatrix} A_1 \\ A_2 \\ G_0 \end{pmatrix} = U^A \begin{pmatrix} \varphi_d \\ \varphi_u \\ \xi \end{pmatrix}, \quad \begin{pmatrix} G^+ \\ H^+ \end{pmatrix} = U^{H^+} \begin{pmatrix} H_d^+ \\ H_u^+ \end{pmatrix}, \tag{8}$$

where $H_{1,2,3}$ and $A_{1,2}$ are respectively the CP-even and CP-odd neutral Higgs bosons, G^0 and G^+ are Goldstone bosons, and H^+ is the charged Higgs boson. So in the NMSSM and nMSSM, there exist a pair of charged Higgs bosons, three CP-even and two CP-odd neutral Higgs bosons. In the MSSM, due to the absence of S, we only have two CP-even and one CP-odd neutral Higgs bosons in addition to a pair of charged Higgs bosons.

The MSSM predict four neutralinos χ_i^0 ($i = 1, 2, 3, 4$), i.e. the mixture of neutral gauginos (bino λ' and neutral wino λ^3) and neutral Higgsinos ($\psi_{H_u}^0, \psi_{H_d}^0$), while the NMSSM and nMSSM predict one more neutralino because the

singlino ψ_S comes into the mixing. In the basis $(-i\lambda', -i\lambda^3, \psi^0_{H_u}, \psi^0_{H_d}, \psi_S)$ (for MSSM ψ_S is absent) the neutralino mass matrix is given by

$$\begin{pmatrix} M_1 & 0 & m_Z s_W s_b & -m_Z s_W c_b \\ 0 & M_2 & -m_Z c_W s_b & m_Z c_W c_b \\ m_Z s_W s_b & -m_Z s_W s_b & 0 & -\mu \\ -m_Z s_W c_b & -m_Z c_W c_b & -\mu & 0 \end{pmatrix} \quad \text{for MSSM} \tag{9}$$

$$\begin{pmatrix} M_1 & 0 & m_Z s_W s_b & -m_Z s_W c_b & 0 \\ 0 & M_2 & -m_Z c_W s_b & m_Z c_W c_b & 0 \\ m_Z s_W s_b & -m_Z s_W s_b & 0 & -\mu & -\lambda v c_b \\ -m_Z s_W c_b & -m_Z c_W c_b & -\mu & 0 & -\lambda v s_b \\ 0 & 0 & -\lambda v c_b & -\lambda v s_b & 2\frac{\kappa}{\lambda}\mu \end{pmatrix} \quad \text{for NMSSM} \tag{10}$$

$$\begin{pmatrix} M_1 & 0 & m_Z s_W s_b & -m_Z s_W c_b & 0 \\ 0 & M_2 & -m_Z c_W s_b & m_Z c_W c_b & 0 \\ m_Z s_W s_b & -m_Z s_W s_b & 0 & -\mu & -\lambda v c_b \\ -m_Z s_W c_b & -m_Z c_W c_b & -\mu & 0 & -\lambda v s_b \\ 0 & 0 & -\lambda v c_b & -\lambda v s_b & 0 \end{pmatrix} \quad \text{for nMSSM} \tag{11}$$

where M_1 and M_2 are respectively $U(1)$ and $SU(2)$ gaugino masses, $s_W = \sin\theta_W$, $c_W = \cos\theta_W$, $s_b = \sin\beta$ and $c_b = \cos\beta$ with $\tan\beta \equiv v_u/v_d$. In our study the lightest neutralino χ^0_1 is assumed to be the lightest supersymmetric particle (LSP), serving as the SUSY dark matter particle. It is composed by

$$\chi^0_1 = N_{11}(-i\lambda_1) + N_{12}(-i\lambda_2) + N_{13}\psi^0_{H_u} + N_{14}\psi^0_{H_d} + N_{15}\psi_S, \tag{12}$$

where N is the unitary matrix (N_{15} is zero for the MSSM) to diagonalize the mass matrix in Eqs.(9-11).

The chargino sector of these three models is the same except that for the NMSSM/nMSSM the parameter μ is replaced by $\mu_{\rm eff}$. The charginos $\chi^\pm_{1,2}$ ($m_{\chi^\pm_1} \leq m_{\chi^\pm_2}$) are the mixture of charged Higgsinos $\psi^\pm_{H_{u,d}}$ and winos $\lambda^\pm = (\lambda^1 \pm \lambda^2)/\sqrt{2}$, whose mass matrix in the basis of $(-i\lambda^\pm, \psi^\pm_{H_{u,d}})$ is given by

$$\begin{pmatrix} M_2 & \sqrt{2}m_W \sin\beta \\ \sqrt{2}m_W \cos\beta & \mu_{\rm eff} \end{pmatrix}. \tag{13}$$

So the chargino $\chi^\pm_1$ can be wino-dominant (when M_2 is much smaller than μ) or Higgsino-dominant (when μ is much smaller than M_2). Since the composing property (wino-like, bino-like, Higgsino-like or singlino-like) of the LSP and the chargino $\chi^\pm_1$ is very important for SUSY phenomenology, we will show such a property in our following study.

III. NUMERICAL RESULTS AND DISCUSSIONS

So far there are various constraints from both collider and dark matter experiments. In our study we consider the following constraints:

(1) Direct bounds on sparticle and Higgs masses from LEP and Tevatron experiments [12], e.g.,$m_{\chi^+_1} > 103.5$ GeV, $m_{\tilde{e}} > 73$ GeV, $m_{\tilde{\mu}} > 94$ GeV, $m_{\tilde{\tau}} > 81.9$ GeV and $m_{H^+} > 78.6$ GeV.

(2) LEP II search for Higgs boson [13], which include various channels of Higgs boson productions [14].

(3) LEP I and LEP II constraints on the productions of neutralinos and charginos, including the LEP I invisible Z-decay $\Gamma(Z \to \chi^0_1\chi^0_1) < 1.76$ MeV, the LEP II neutralino production $\sigma(e^+e^- \to \chi^0_1\chi^0_i) < 10^{-2}$ pb ($i > 1$) and $\sigma(e^+e^- \to \chi^0_i\chi^0_j) < 10^{-1}$ pb.

(4) Indirect constraints from precision electroweak observables such as ρ_ℓ, $\sin^2\theta^\ell_{eff}$ and M_W, or their combinations $\epsilon_i (i = 1, 2, 3)$ [15]. We require ϵ_i to be compatible with the LEP/SLD data at 95% confidence level. Also, for $R_b = \Gamma(Z \to b\bar{b})/\Gamma(Z \to \text{hadrons})$ whose measured value is $R^{exp}_b = 0.21629 \pm 0.00066$ and the SM prediction is $R^{SM}_b = 0.21578$ for $m_t = 173$ GeV [12], we require R^{SUSY}_b is within the 2σ range of its experimental value. Various B-physics constraints are also included [14].

(5) Indirect constraint from the muon anomalous magnetic moment, $a^{exp}_\mu - a^{SM}_\mu = (25.5 \pm 8.0) \times 10^{-10}$ [16], for which we require the SUSY effects to account at 2σ level. (We note that 3σ effects are considered to be inconclusive

in high energy physics. In collider experiments, there are a large number of channels and observables and there is a good chance that some of the measurements can show such deviation from expectation. The muon $g-2$ experiment is quite different because there is just one quantity to measure in the experiment. In our opinion, the significance of the deviation should be taken rather seriously.)

(6) Dark matter constraints from the WMAP relic density $0.0945 < \Omega h^2 < 0.1287$ [17] and CDMS II limits on the scattering cross section [8]. To show the effects of the CDMS II limits, we will display the results with/without such limits.

In addition to the above experimental limits, we also consider the constraint from the stability of the Higgs potential, which requires that the physical vacuum of the Higgs potential with non-vanishing vevs of Higgs scalars should be lower than any local minima. Further, the soft breaking parameters are required to be below 1 TeV to avoid the fine-tuning, and λ (at weak scale) is less than about 0.7 to ensure perturbativity of the theory up to the grand unification scale (λ is increasing with the energy scale [18]). Note that most of these constraints have been encoded in NMSSMTools [14]. We extend this package and use it in our calculations. For the cross section of χ-nucleon scattering, we use the formulas in [19, 20] for the MSSM and extend them to the NMSSM/nMSSM (see Appendix A).

Considering all the constraints listed above, we scan over the parameters in the following ranges

$$\begin{aligned} &100\ \text{GeV} \leq \left(M_{\text{soft}}^{\text{squark}}, M_{\text{soft}}^{\text{slepton}},\ m_A,\ \mu\right) \leq 1\ \text{TeV}, \\ &50\ \text{GeV} \leq M_1 \leq 1\ \text{TeV},\quad 1 \leq \tan\beta \leq 40, \\ &(|\lambda|, |\kappa|) \leq 0.7,\quad |A_\kappa| \leq 1\ \text{TeV}, \end{aligned} \tag{14}$$

To reduce the number of the relevant soft parameters, we work in the so-called m_h^{max} scenario with following choice of the soft masses for the third generation squarks: $M_{Q_3} = M_{U_3} = M_{D_3} = 800$ GeV, and $X_t = A_t - \mu \cot\beta = -1600$ GeV. The advantage of such a choice is that other SUSY parameters are easy to survive the constraints (so that the bounds we obtain are conservative). Moreover, we assume the grand unification relation for the gaugino masses: $M_1 : M_2 : M_3 \simeq 1 : 1.83 : 5.26$ and also assume universal masses $M_{\tilde{\ell}}$ and $M_{\tilde{q}}$ for the three generations of sleptons and the first two generations of squarks respectively.

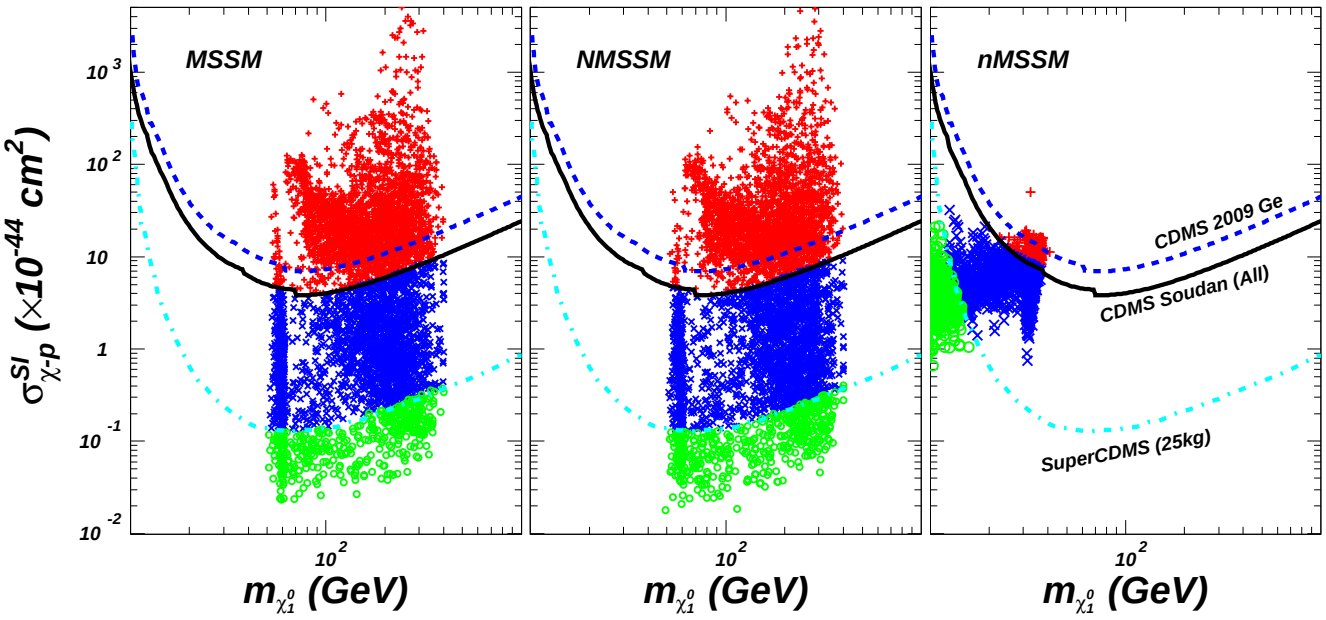

FIG. 1: The scatter plots for the spin-independent elastic cross section of χ-nucleon scattering. The '+' points (red) are excluded by CDMS limits (solid line), the '$\times$' (blue) would be further excluded by SuperCDMS 25kg [11] in case of unobservation (dash-dotted line), and the '$\circ$' (green) are beyond the SuperCDMS sensitivity.

The surviving points are displayed in Fig. 1 for the spin-independent elastic cross section of χ-nucleon scattering. We see that for each model the CDMS II limits can exclude a large part of the parameter space allowed by current collider constraints and the future SuperCDMS (25 kg) can cover the most part of the allowed parameter space. For the MSSM and NMSSM the dark matter mass range $m_{\chi_1^0}$ is from 50 GeV to 400 GeV, while for the nMSSM

the dark matter mass is constrained below 40 GeV by current experiments and further constrained below 20GeV by SuperCDMS in case of unobservation. For the MSSM/NMSSM the LSP lower bound at 50 GeV is from the chargino lower bound of 103.5 GeV plus the assumed GUT relation $M_1 \simeq 0.5M_2$; while the upper bound at 400 GeV is from the bino nature of the LSP (M_1 cannot be too large, must be much smaller than other relevant parameters) plus the constraints from the LEP II search for Higgs bosons, the muon g-2 and B-physics. Note that if we do not assume the GUT relation $M_1 \simeq 0.5M_2$, then M_1 can be as small as 40 GeV and the LSP lower bound in MSSM/NMSSM will not be sharply at 50 GeV.

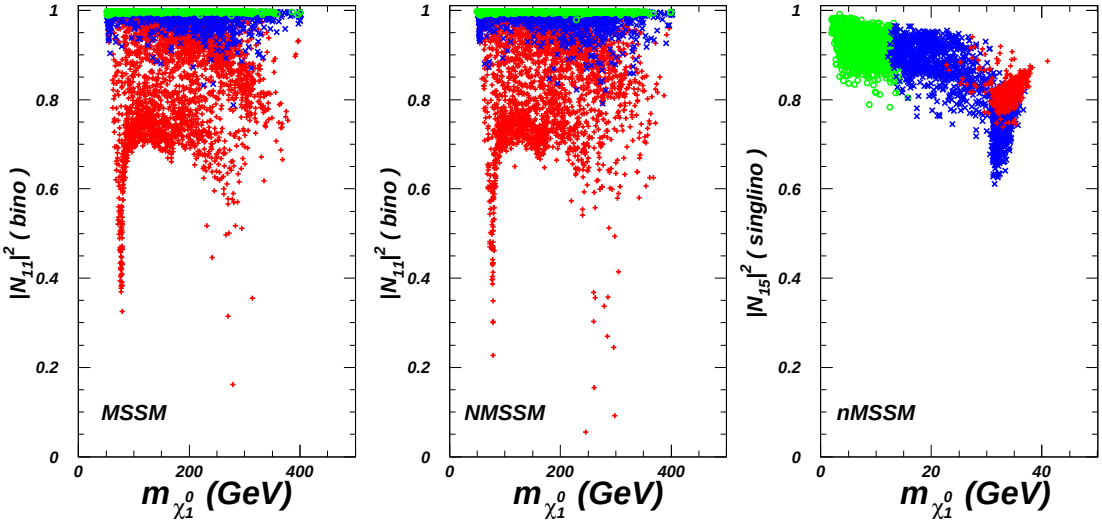

FIG. 2: Same as Fig. 1, but projected on the plane of $|N_{11}|^2$ and $|N_{15}|^2$ versus dark matter mass.

In Fig. 2 we show the bino component of χ_1^0 in MSSM/NMSSM and the singlino component of χ_1^0 in nMSSM. We see that for both the MSSM and NMSSM χ_1^0 is bino-dominant, while for the nMSSM χ_1^0 is singlino-dominant, and the region allowed by CDMS limits (and SuperCDMS limits in case of unobservation) favor a more bino-like χ_1^0 for the MSSM/NMSSM and a more singlino-like χ_1^0 for the nMSSM. For the MSSM/NMSSM, the reason is obvious because the dominant contribution to the cross section comes from Fig. 9 in the Appendix and a more bino-like χ_1^0 tends to suppress not only $f_{q_i}^{\tilde{q}}$ in Eq.(A3) [20], but also $f_{q_i}^H$ by diminishing T_{h00}. As for the nMSSM, χ_1^0 is singlino-like due to the small singlino mass in the neutralino mass matrix. The peculiarity of the nMSSM predictions will be discussed at the end of this section.

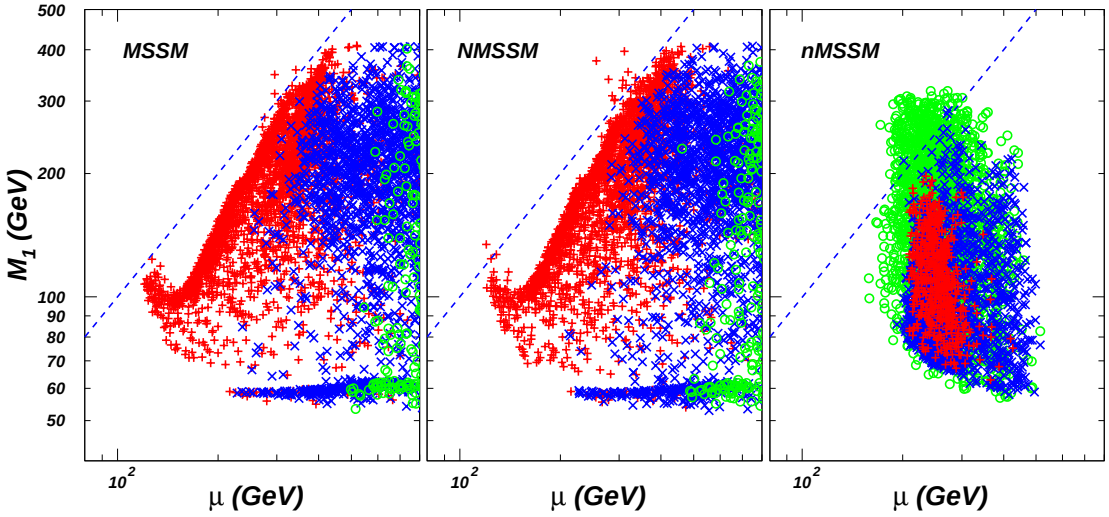

FIG. 3: Same as Fig. 1, but projected on the plane of M_1 versus μ. The dashed lines are for $M_1 = \mu$.

In Fig. 3 we project the surviving points on the plane of M_1 versus μ. We see that for both the MSSM and NMSSM most of the survived points are below the $M_1 = \mu$ line, implying that χ_1^0 is bino-dominant. The region allowed by

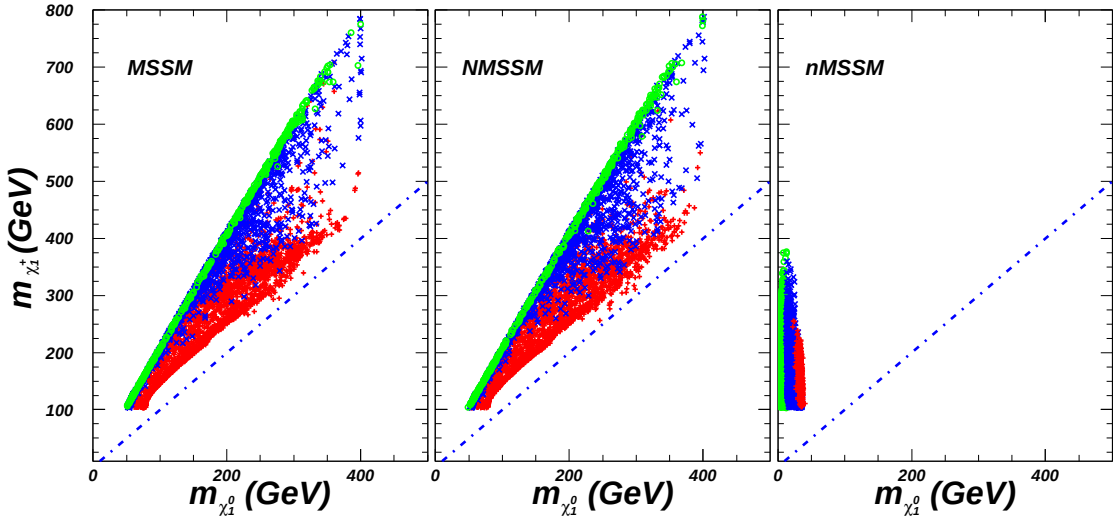

FIG. 4: Same as Fig. 1, but showing the chargino mass $m_{\chi_1^+}$ versus the LSP mass. The dashed lines indicate $m_{\chi_1^+} = m_{\chi_1^0}$.

the CDMS limits tends to have a larger μ, indicating a more bino-like χ_1^0, which can be inferred from the neutralino mass matrices in Eq.(11). For the nMSSM the upper bound of 500 GeV for μ is from the fact that a larger μ leads to a lighter LSP (as will be shown in Eq.15), which is then constrained by the required annihilation rate of the LSP.

In Fig. 4 we display the surviving points on the plane of the chargino mass $m_{\chi_1^+}$ versus $m_{\chi_1^0}$. For both the MSSM and NMSSM, the CDMS limits tend to favor a heavier chargino and ultimately the SuperCDMS limits tend to favor a wino-dominant chargino with mass about $2m_{\chi_1^0}$. This can be understood because the CDMS/SuperCDMS limits require a large μ, which makes χ_1^+ to be dominated by wino with a mass $M_2 \simeq 2M_1$.

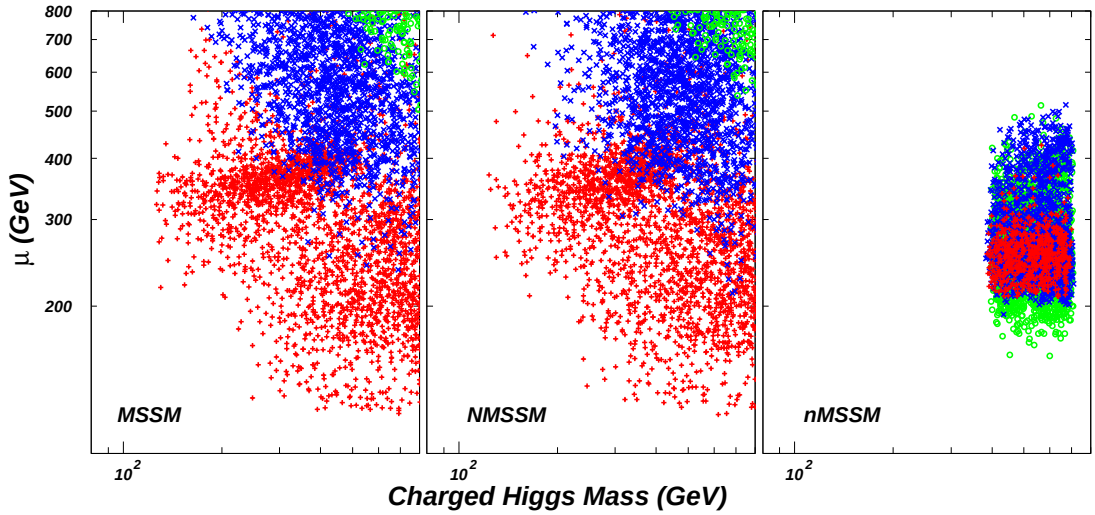

FIG. 5: Same as Fig. 1, but projected on the plane of μ versus the charged Higgs mass.

In Figs.5 and 6 we display the surviving points on the plane of μ and $\tan\beta$ versus the charged Higgs mass. In both the MSSM and NMSSM, large μ and small $\tan\beta$ are favored for a light charged Higgs boson. The reason is as follows. In the MSSM, there are two CP-even Higgs bosons contributing to the cross section. One is the SM-like Higgs boson h^0 with mass around 120GeV and the other is the heavy boson H^0 with mass nearly degenerate with the charged Higgs boson. Then from the expression of $f_{q_i}^H$ in Eq.(A3), one can learn that the H^0 contribution to the scattering cross section get enhanced for light charged Higgs boson. In this case, to alleviate such enhancement, large μ (to lower T_{H00}) and/or small $\tan\beta$ (to lower $T_{hq_iq_i}$) are needed. In the NMSSM, although there are three CP-even Higgs boson contributing to the scattering, we can get the same conclusion as the MSSM because one of the bosons is singlet-dominant and its contribution is suppressed by $T_{hq_iq_i}$, and the contributions from the other two bosons are quite similar to the case of the MSSM, .

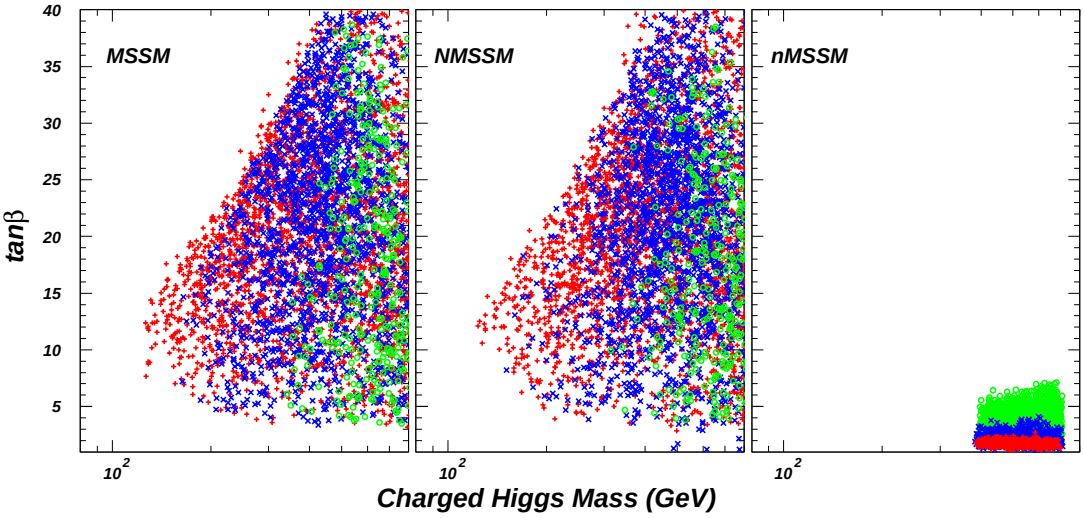

FIG. 6: Same as Fig. 1, but projected on the plane of $\tan\beta$ versus the charged Higgs mass.

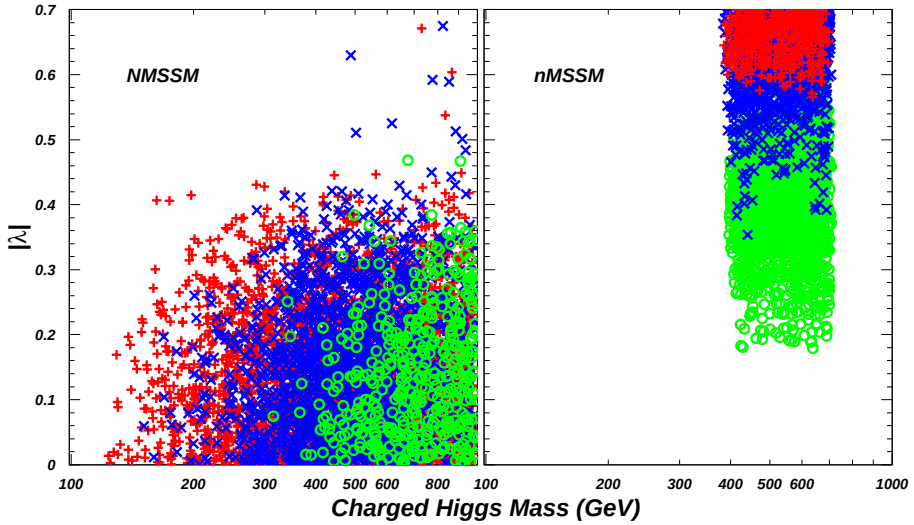

FIG. 7: Same as Fig. 1, but projected on the plane of $|\lambda|$ versus the charged Higgs mass in NMSSM and nMSSM.

In Fig. 7 we show the value of $|\lambda|$ versus the charged Higgs mass in NMSSM and nMSSM. This figure indicates that λ larger than 0.4 is disfavored for the NMSSM. The underlying reason is that T_{h00} in Eq.(A3) depends on λ explicitly and large λ can enhance T_{h00} [14]. By contrast, although CDMS has excluded some points with large λ in the nMSSM, there are still many surviving points with λ as large as 0.7.

In Fig. 8 we show the decay branching ratio of $h^0 \to \chi_1^0\chi_1^0$ versus the mass of the SM-like Higgs boson h^0. Such a decay is strongly correlated to the χ-nucleon scattering because the coupling $h^0\chi_1^0\chi_1^0$ is involved in both processes. We see that in the MSSM and NMSSM this decay mode can open only in a very narrow parameter space since χ_1^0 cannot be so light, and in the allowed region this decay has a very small branching ratio (below 10%). By contrast, in the nMSSM this decay can open in a large part of the parameter space since the LSP can be very light, and its branching ratio can be quite large (over 80% or 90%). Such a large invisible decay ratio may indicate a severe challenge for finding the Higgs boson h^0 at the LHC if the nMSSM is the true story. Fig. 8 also indicates that the mass of h^0 can reach 160 GeV. We checked that these cases correspond to λ varying from 0.6 to 0.7 so that the mass is enhanced at tree level.

Now we discuss the reason for the peculiarity of the nMSSM predictions shown from Fig. 2 to Fig. 8. About the narrow parameter space of the nMSSM constrained by collider experiments, a detailed analysis has been given in [4], here we only explain the behavior of the nMSSM under the CDMS/SuperCDMS limits. Our explanation is based on following three facts. The first comes from the neutralino mass matrix in Eq.(11) which implies that $m_{\chi_1^0}$ can be

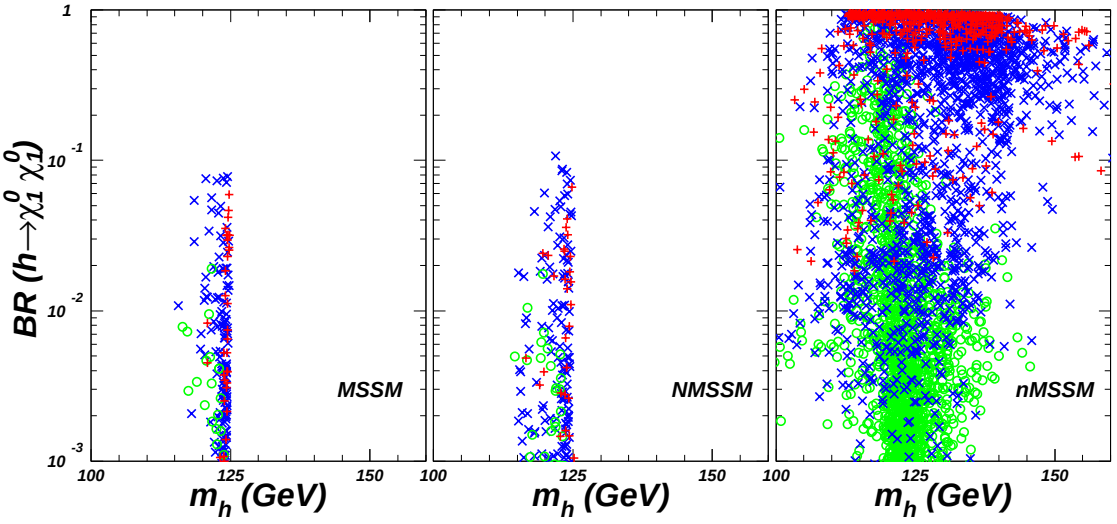

FIG. 8: Same as Fig. 1, but projected for the decay branching ratio of $h^0 \to \chi_1^0\chi_1^0$ versus the mass of the Higgs boson h (the SM-like Higgs boson).

written as [4]:

$$m_{\chi_1^0} \simeq \frac{2\mu\lambda^2(v_u^2+v_d^2)}{2\mu^2+\lambda^2(v_u^2+v_d^2)}\frac{\tan\beta}{\tan^2\beta+1}. \tag{15}$$

This formula shows that to get a heavy χ_1^0, we need a large λ, a small $\tan\beta$ as well as a moderate μ. The second fact is that, due to the singlino dominance of χ_1^0 in the nMSSM, the interaction of χ_1^0 with squarks is suppressed and the Higgs mediated contribution in Figs.9 and 10 then becomes dominant in the scattering. In this case, λ determines the size of the scattering for a given $m_{\chi_1^0}$ by affecting the coupling T_{h00} [14] and a large λ can enhance the cross section. The last fact is based on Fig. 1 which shows that the constraints of CDMS results become stringent for heavy $\tilde{\chi}_1^0$ and as a result, only $m_{\tilde{\chi}_1^0}$ around 40 GeV is excluded by CDMS. With these facts, one can easily understand the features of Figs. 2-8. For example, Fig. 6 and Fig. 7 indicate that the disfavored points by CDMS are characterized by small $\tan\beta$ and large λ. The reason is that only under these two conditions, both $m_{\tilde{\chi}}$ and the cross section can be large simultaneously.

The similarity of the allowed parameter space for the MSSM and NMSSM can be understood as follows. In both models χ_1^0 is composed dominantly by bino, as shown in Fig. 2. Then the properties of χ_1^0 (like the relic density and the χ-nucleon scattering) are similar in both models. Our such conclusion agrees with [21] except that the conclusion of [21] is based on a different scan scheme. Compared with [21], we considered more constraints and so our conclusions are more robust.

IV. SUMMARY

Considering the current direct and indirect collider constraints, we gave a comparative study for the neutralino dark matter scattering on nucleon in the MSSM, the NMSSM and the nMSSM. We showed the predictions for the elastic cross section by scanning over the parameter space allowed by the collider constraints and demonstrated the property of the allowed parameter space with/without the new limits from CDMS II. We found that for each model the new CDMS limits can exclude a large part of parameter space allowed by current collider constraints. The property of the allowed parameter space is found to be similar for MSSM and NMSSM, but quite different for nMSSM. Further, the future SuperCDMS can cover most part of the allowed parameter space for each model.

Acknowledgment

This work was supported in part by HASTIT under grant No. 2009HASTIT004, by the Grant-in-Aid for Scientific Research (No. 14046201) from the Japan Ministry of Education, Culture, Sports, Science and Technology, by the National Natural Science Foundation of China (NNSFC) under grant Nos. 10505007, 10821504, 10725526 and

10635030, and by the Project of Knowledge Innovation Program (PKIP) of Chinese Academy of Sciences under grant No. KJCX2.YW.W10.

Appendix A: Spin-Independent Cross section of χ-nucleon scattering

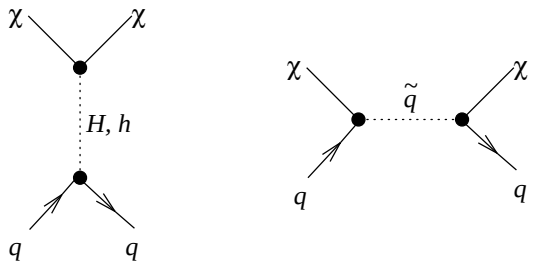

FIG. 9: Feynman diagrams contributing to the scalar elastic-scattering amplitude of a neutralino from quarks in the MSSM, where H and h denote the CP-even Higgs bosons and $\tilde{q}$ represents a scalar quark.

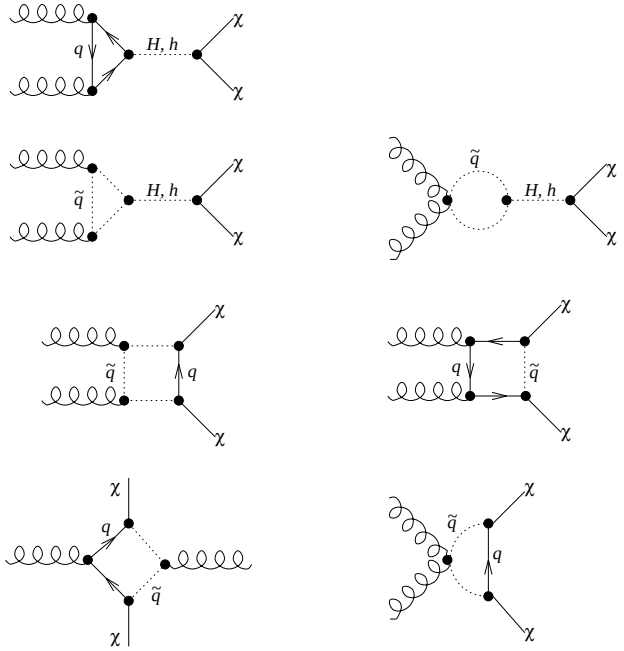

FIG. 10: Feynman diagrams contributing to the gluonic interaction with neutralinos, which contributes to the scalar elastic-scattering amplitude for neutralinos and nuclei.

In supersymmetric models, the spin-independent elastic χ-nucleon scattering is described by the following effective Lagrangian[19, 20]:

$$\begin{aligned}\mathcal{L} &= f_q \bar{\chi}\chi\bar{q}q + g_q\left[-2i\bar{\chi}\gamma^\mu\partial^\nu\chi\mathcal{O}^{(2)}_{q\mu\nu} - \frac{1}{2}m_q m_\chi \bar{q}q\bar{\chi}\chi\right] \\ &\quad + b\,\alpha_s\bar{\chi}\chi G^a_{\mu\nu}G^{a\mu\nu} - \alpha_s(B_{1D}+B_{1S})\bar{\chi}\partial_\mu\partial_\nu\chi\,\mathcal{G}^{(2)\mu\nu} \\ &\quad + \alpha_s B_{2S}\bar{\chi}\left(i\partial_\mu\gamma_\nu + i\partial_\nu\gamma_\mu\right)\chi\,\mathcal{G}^{(2)\mu\nu}, \end{aligned} \tag{A1}$$

where the twist-two quark and gluon operators are defined by

$$\begin{aligned}\mathcal{O}^{(2)}_{q\mu\nu} &= \frac{i}{2}\left[\bar{q}\gamma_\mu\partial_\nu q + \bar{q}\gamma_\nu\partial_\mu q - \frac{1}{2}g_{\mu\nu}\bar{q}\,\partial\!\!\!/ q\right], \\ \mathcal{G}^{(2)\mu\nu} &= G^{a\mu}_\rho G^{a\rho\nu} + \frac{1}{4}g^{\mu\nu}G^{a\sigma\rho}G^a_{\sigma\rho}, \end{aligned} \tag{A2}$$

$G_a^{\mu\nu}$ is the gluon field-strength tensor, and f_q, g_q, b and B are coefficients.

In the MSSM, the coefficients f_q and q_q are determined by calculating the diagrams in Fig. 9 in the extreme nonrelativistic limit, and they are given by

$$\begin{aligned} f_{q_i} &= f_{q_i}^{\tilde{q}} + f_{q_i}^{H} = -\frac{1}{4}\sum_{\tilde{q}_j} \frac{X'_{q\ ij\,0} W'_{q\ ij\,0}}{m^2_{\tilde{q}_j} - (m_\chi + m_{q_i})^2} \ + \sum_{h=h^0,H^0} \frac{g T_{h00} T_{h q_i q_i}}{2 m_h^2}, \\ g_{q_i} &= -\frac{1}{8}\sum_{\tilde{q}_j} \frac{\left(X'_{q\ ij\,0}\right)^2 + \left(W'_{q\ ij\,0}\right)^2}{\left[m^2_{\tilde{q}_j} - (m_\chi + m_{q_i})^2\right]^2}, \end{aligned} \tag{A3}$$

where the subscripts $q = u, d$ and $i = 1, 2, 3$ refers to the flavor index in quark sector, and X'_{qij0}, W'_{qij0}, T_{h00} and $T_{hq_iq_i}$ are the coupling coefficients of $\bar{q}_i P_R \chi_0 \tilde{q}_j$, $\bar{q}_i P_R \chi_0 \tilde{q}_j$, $\bar{\chi}_0 \chi_0 h$ and $\bar{q}_i q_i h$ vertices respectively.

The coefficients of the last four operators can be obtained in a similar way from Fig. 10, and their expressions are

$$\begin{aligned} b &= -T_{\tilde{q}} + B_D + B_S - \frac{m_\chi}{2} B_{2S} - \frac{m_\chi^2}{4}(B_{1D} + B_{1S}), \\ T_{\tilde{q}} &= \frac{1}{96\pi} \sum_{h=h^0,H^0} \frac{g}{2} \frac{T_{h\,00}}{m_h^2} \sum_{\tilde{q}_j} \frac{g_{h\tilde{q}_j\tilde{q}_j}}{m^2_{\tilde{q}_j}} \\ B_D &= \frac{1}{32\pi} \sum_{q_i,\tilde{q}_j} m_{q_i} X'_{q\ ij\,0} W'_{q\ ij\,0}\ I_1(m_{q_i}, m_{\tilde{q}_j}, m_\chi), \\ B_S &= \frac{1}{32\pi} \sum_{q_i,\tilde{q}_j} m_\chi \frac{1}{2} \left[\left(X'_{q\ ij\,0}\right)^2 + \left(W'_{q\ ij\,0}\right)^2\right]\ I_2(m_{q_i}, m_{\tilde{q}_j}, m_\chi), \\ B_{1D} &= \frac{1}{12\pi} \sum_{q_i,\tilde{q}_j} m_{q_i} X'_{q\ ij\,0} W'_{q\ ij\,0}\ I_3(m_{q_i}, m_{\tilde{q}_j}, m_\chi), \\ B_{1S} &= \frac{1}{12\pi} \sum_{q_i,\tilde{q}_j} m_\chi \frac{1}{2} \left[\left(X'_{q\ ij\,0}\right)^2 + \left(W'_{q\ ij\,0}\right)^2\right]\ I_4(m_{q_i}, m_{\tilde{q}_j}, m_\chi), \\ B_{2S} &= \frac{1}{48\pi} \sum_{q_i,\tilde{q}_j} \frac{1}{2} \left[\left(X'_{q\ ij\,0}\right)^2 + \left(W'_{q\ ij\,0}\right)^2\right]\ I_5(m_{q_i}, m_{\tilde{q}_j}, m_\chi), \end{aligned} \tag{A4}$$

where I_ks are functions given in Eqs. (B.1a-e) of [20] with the Eq. (B.1d) corrected as follows: the factor in the first term should read $(m_{\tilde{q}}^2 - m_q^2 - m_\chi^2)$, with a corrected exponent for m_χ; the term immediately following should read $-1/m_{\tilde{q}}^2 m_\chi^4$, again with a corrected exponent for m_χ; finally, a sign in the last term should be corrected so that it reads $\left[\cdots - m_{\tilde{q}}^2 + m_\chi^2\right] L$.

About above formulae, two points should be noted. One is the Lagrangian in Eq.(A1) is specified at a high-energy scale, for example, $\mu_0 \simeq m_h$, and in order to get the scattering rate measured in dark matter direct detection experiments, one must consider important QCD and SUSY-QCD corrections to the coefficients[22]. In our calculation, we have considered such effect. The other is some extensions of the MSSM, such as NMSSM and nMSSM considered in this paper, usually predict extra CP-even Higgs bosons and neutralinos, and consequently, the couplings appeared in above formulae may be changed. In this case, the formulae listed above still keep valid in the sense that one must use the corresponding new couplings with the same convention as that in[19] and also include the contributions from new intermediate states. For example, the NMSSM predicts three CP-even Higgs bosons, and one should add the three boson contributions in getting $f_{q_i}^H$[23].

Given the effective Lagrangian in Eq.(A1), one can write down the spin-independent scattering cross section of a neutralino from a nucleon N (proton or neutron) in a standard way[20, 24]:

$$\sigma^{SI} = \frac{4 m_r^2}{\pi} f_N^2 \tag{A5}$$

where $m_r = \frac{m_\chi m_N}{m_\chi + m_N}$ is the reduced LSP mass, and f_N is the effective couplings of the neutralino to nucleon, which

is given by:

$$\frac{f_N}{m_N} = \sum_{q=u,d,s} \frac{f_{Tq}^N}{m_q}\left[f_q - \frac{m_\chi m_q}{2} g_q\right] + \frac{2}{27} f_{TG}^N \sum_{q=c,b,t} \frac{f_q^H}{m_q} - \frac{3}{2} m_\chi \sum_{q=u,d,s,c,b} g_q(\mu_0) q^N(\mu_0^2) - \frac{8\pi}{9}\, b\, f_{TG}^N + \frac{3}{2} m_\chi G^N(\mu_0^2)\alpha_s(\mu_0^2)\left[B_{2S} + \frac{m_\chi}{2}\left(B_{1D} + B_{1S}\right)\right]. \quad \text{(A6)}$$

In Eq.(A6), f_{Tq}^N denotes the fraction of the nucleon mass m_N that is due to the light quark q, and $f_{TG}^N = \frac{2}{27}(1 - f_{Tu}^N - f_{Td}^N - f_{Ts}^N)$ is the heavy quark contribution to m_N, which is induced via gluon exchange. The function $q^N(\mu_0^2)$ and $G^N(\mu_0^2)$ appear in the second moment of the quark (gluon) distribution functions and they represent the quark and gluon densities in the nucleon at the scale μ_0. The quantities $g_q(\mu_0)q^N(\mu_0^2)$ and $G^N(\mu_0^2)\alpha_s(\mu_0^2)$ in the third term and the last term is a renormalization-group invariant (in other words, independent of μ_0) and their evaluation was described in detail in [20]. In our calculation, we use $\sigma_{\pi N} = 64$ MeV and $\sigma_0 = 35$ MeV to get the values of f_{Tq}^N and use CTEQ6L to get the values of $q^N(m_b^2)$ and $G^N(m_t^2)$.

Before we end this section, we remind two subtleties in Eq.(A6)[20]. One is to get the coefficient b by the formula in Eq.(A4), one should not include the contribution of u, d, s quarks to B_D since they are non-perturbative effects. The other is only top quark contribution needs to be considered in getting B_{2S} in the last term. The reason is the contributions from u, d, s quarks to B_{2S} are non-perturbative effects, and the contributions from c, b quarks have been moved to the third term of Eq.(A6).

[1] For a review, see, e.g., H. E. Haber and G. L. Kane, Phys. Rept. **117**, 75 (1985).

[2] See, e.g., J. R. Ellis, *et al.*, Phys. Rev. D **39**, 844 (1989); M. Drees, Int. J. Mod. Phys. A **4**, 3635 (1989). S. F. King, P. L. White, Phys. Rev. D **52**, 4183 (1995); B. Ananthanarayan, P.N. Pandita, Phys. Lett. B **353**, 70 (1995); Phys. Lett. B **371**, 245 (1996); Int. J. Mod. Phys. A12, 2321 (1997); B. A. Dobrescu, K. T. Matchev, JHEP **0009**, 031 (2000); V. Barger, P. Langacker, H.-S. Lee, G. Shaughnessy, Phys. Rev. D **73**,(2006) 115010; R. Dermisek, J. F. Gunion, Phys. Rev. Lett. **95**, 041801 (2005); G. Hiller, Phys. Rev. D **70**, 034018 (2004); F. Domingo, U. Ellwanger, JHEP **0712**, 090 (2007); Z. Heng, *et al.*, Phys. Rev. D **77**, 095012 (2008); R. N. Hodgkinson, A. Pilaftsis, Phys. Rev. D **76**, 015007 (2007); Phys. Rev. D **78**, 075004 (2008); W. Wang, Z. Xiong, J. M. Yang, Phys. Lett. B **680**, 167 (2009); J. Cao, J. M. Yang, JHEP **0812**, 006 (2008); Phys. Rev. D **78**, 115001 (2008);

[3] P. Fayet, Nucl. Phys. B **90**, 104 (1975); C. Panagiotakopoulos, K. Tamvakis, Phys. Lett. B **446**, 224 (1999); Phys. Lett. B **469**, 145 (1999); C. Panagiotakopoulos, A. Pilaftsis, Phys. Rev. D **63**, 055003 (2001); A. Dedes, *et al.*, Phys. Rev. D **63**, 055009 (2001); A. Menon, *et al.*, Phys. Rev. D **70**, 035005 (2004); V. Barger, *et al.*, Phys. Lett. B **630**, 85 (2005). C. Balazs, *et al.*, JHEP **0706**, 066 (2007).

[4] J. Cao, H. E. Logan, J. M. Yang, Phys. Rev. D **79**, 091701 (2009).

[5] D. Hooper and T. M. P. Tait, Phys. Rev. D **80**, 055028 (2009); W. Wang, *et al.*, JHEP **0911**, 053 (2009); Y. Bai, M. Carena, J. Lykken, arXiv:0905.2964.

[6] O. Adriani *et al.*, PAMELA Collaboration, Nature **458**, 607 (2009).

[7] O. Lebedev and S. Ramos-Sanchez, arXiv:0912.0477.

[8] Z. Ahmed, *et al.*, CDMS-II Collaboration, arXiv:0912.3592.

[9] For recent works motivated by CDMS II results, see, e.g., M. Kadastik, K. Kannike, A. Racioppi and M. Raidal, arXiv:0912.3797; N. Bernal and A. Goudelis, arXiv:0912.3905; A. Bottino, F. Donato, N. Fornengo and S. Scopel, arXiv:0912.4025; D. Feldman, Z. Liu and P. Nath, arXiv:0912.4217; M. Ibe and T. T. Yanagida, arXiv:0912.4221; R. Allahverdi, B. Dutta and Y. Santoso, arXiv:0912.4329; M. Endo, S. Shirai and K. Yonekura, arXiv:0912.4484; Q. H. Cao, I. Low and G. Shaughnessy, arXiv:0912.4510; Q. H. Cao, C. R. Chen, C. S. Li and H. Zhang, arXiv:0912.4511; K. Cheung and T. C. Yuan, arXiv:0912.4599; J. Hisano, K. Nakayama and M. Yamanaka, arXiv:0912.4701; X. G. He, *et al.*, arXiv:0912.4722; I. Gogoladze, R. Khalid, S. Raza and Q. Shafi, arXiv:0912.5411; M. Aoki, S. Kanemura and O. Seto, arXiv:0912.5536; R. Foot, arXiv:1001.0096; M. Asano and R. Kitano, arXiv:1001.0486; W. S. Cho et al., arXiv:1001.0579; J. Shu, P. F. Yi, S. H. Zhu, arXiv:1001.1076; D. P. Roy, arXiv:1001.4346; S. Khalil, H. S. Lee, E. Ma, arXiv:1002.0692; A. Bandyopadhyay, *et al.*, arXiv:1002.0753; arXiv:1003.0809; J. Hisano, *et al.*, arXiv:1003.3648; L. Wang, J. M. Yang, arXiv:1003.4492.

[10] J. Ellis, A. Ferstl and K. A. Olive, Phys. Lett. B **481**, 304 (2000); J. Ellis, K. A. Olive, Y. Santoso, V. C. Spanos, Phys. Rev. D **71**, 095007 (2005); A. Bottino, *et al.*, Phys. Lett. B **402**, 113 (1997).

[11] R. Gaitskell, V. Mandic, and J. Filippini, http://dmtools.berkeley.edu/limitplots.

[12] C. Amsler, *et al.* (Particle Data Group), Phys. Lett. B **667**, 1 (2008).

[13] S. Schael, *et al.*, Eur. Phys. Jour. C **47**, 547 (2006).

[14] U. Ellwanger, J. F. Gunion and C. Hugonie, JHEP **0502**, 066 (2005); U. Ellwanger and C. Hugonie, Comput. Phys. Commun. **175**, 290 (2006).
[15] G. Altarelli and R. Barbieri, Phys. Lett. B **253**, 161 (1991); M. E. Peskin, T. Takeuchi, Phys. Rev. D **46**, 381 (1992).
[16] M. Davier, *et al.*, Eur. Phys. Jour. C **66**, 1 (2010).
[17] C. L. Bennett *et al.*, Astrophys. J. Suppl. **148** (2003) 1; D. N. Spergel *et al.*, Astrophys. J. Suppl. **148** (2003) 175.
[18] D.J. Miller, R. Nevzorov, P.M. Zerwas, Nucl. Phys. B **681**, 3 (2004).
[19] G. Junman, M. Kamionkowski and K. Griest, Phys. Rept. 267, 195 (1996).
[20] M. Drees and M. Nojiri, Phys. Rev. D **48**, 3483 (1993).
[21] V. Barger, *et al.*, Phys. Rev. D **75**, 115002 (2007).
[22] A. Djouadi and M. Drees, Phys. Lett. B **484**, 183 (2000).
[23] V. A. Bednyakov and H. V. Klapdor-Kleingrothaus, Phys. Rev. D **59**, 023514 (1999); D. G. Cerdeno, *et al.*, JHEP **0412**, 048 (2004); G. Belanger, C. Hugonie and A. Pukhov, JCAP **0901**, 023 (2009).
[24] G. Belanger, F. Boudjema, A. Pukhov and A. Semenov, Comput. Phys. Commun. **180**, 747 (2009).